Carbohydrate Polymers 82 (2010) 264–269

Contents lists available at ScienceDirect

Carbohydrate Polymers

journal homepage: www.elsevier.com/locate/carbpol

Complex formation between amylomaize dextrin and *n*-butanol by phase separation system

Jong-Yea Kim, Seung-Taik Lim*

School of Life Sciences and Biotechnology, Korea University, 5-1, Anam-dong, Sungbuk-ku, Seoul 136-701, Republic of Korea

ARTICLE INFO

Article history:
Received 14 January 2010
Received in revised form 14 April 2010
Accepted 16 April 2010
Available online 29 April 2010

Keywords:
Amylose
n-Butanol
Complex
V-dextrin
Phase separation

ABSTRACT

Crystalline dextrin–butanol particles were prepared through a complex formation using separated phases of an aqueous dextrin solution and *n*-butanol. The dextrin concentration and temperature for the complex formation were important parameters to determine the matrix structure of the complex. When dextrin concentration was relatively high (2 or 3%) and the temperature was low (25 °C), amorphous or B-type crystalline particles were produced. However, at a lower dextrin concentration (1%) and a higher temperature (50 or 70 °C), V_H crystalline particles with *d*-spacings of 1.123, 0.657, and 0.429 nm were produced. Mechanical stirring during the complex formation resulted in smaller size (less than 200 nm) and higher yield (more than 50% based on dextrin) of the complex. The complex particles had rectangular shapes with sizes less than 200 nm, and mainly consisted of long and linear dextrins.

© 2010 Elsevier Ltd. All rights reserved.

1. Introduction

Amylose is a relatively linear polysaccharide composed of α-(1, 4) linked anhydro-glucopyranosyl units. It can self-assemble or crystallize in aqueous media simply by changing the temperature or amylose concentration. Allomorphs of amylose are affected by the solvents used, chain conformation and concentration of amylose, and storage temperature (Gidley & Bulpin, 1989). Cooling a dilute solution containing amylose and a slow diffusion of acetone vapors to amylose solution resulted in the formation of B or A type crystals, respectively (Putaux et al., 2008). In both crystals, 6-folded left-hand amylose double helices are arranged in parallel, but the arrangement pattern of the helices is different. The double helices in the A allomorph are packed in a monoclinic unit cell containing 4 water molecules (Imberty, Chanzy, Pérez, Buléon, & Tran, 1988), whereas those of the B allomorph are packed in a hexagonal unit cell containing 36 water molecules (Imberty & Perez, 1988).

Amylose also forms single helices by accommodating hydrophobic guest molecules inside the helices, which are laterally stacked and form a crystal, the so-called V-amylose. The crystal is classified into several families depending on morphology and electron diffraction diagrams (Cardoso et al., 2007). Hexagonal crystals of V_H type, which results from crystallizing with either fatty acid or hot ethanol (Brisson, Chanzy, & Winter, 1991; Godet, Tran, Delage, & Buléon, 1993; Welland & Donald, 1991; Whittam et al., 1989), have left-handed single helices consisting of 6 anhydroglucopyranosyl units per turn with a pitch of 0.805 nm (Rappenecker & Zugenmaier, 1981). Rectangular crystals, which have a generic name of $V_{butnaol}$, result from the addition of *n*-butanol (Helbert & Chanzy, 1994). Different types of rectangular crystals, which are called $V_{isopropanol}$, can be prepared by the addition of isopropanol or ketones, as well as a large number of complexing agents (Buléon, Delage, Brisson, & Chanzy, 1990; Nuessli, Putaux, Bail, & Buléon, 2003). Square $V_{glycerol}$ crystals, whose diffraction exhibits a near tetragonal symmetry, are formed from high temperature crystallization of amylose with the addition of glycerol (Hulleman, Helbert, & Chanzy, 1996). Also, $V_{naphthol}$ crystals with a tetragonal diffractogram can be obtained with bulky complex agents such as naphthol (Cardoso et al., 2007). It has been considered that $V_{butnaol}$, $V_{isopropanol}$, $V_{naphthol}$ and $V_{glycerol}$ crystals also consist of left-handed 6-fold amylose helices (Booy, Chanzy, & Sarko, 1979; Buléon et al., 1990; Helbert & Chanzy, 1994; Hulleman et al., 1996; Manley, 1964), whereas $V_{naphthol}$ crystal contains 8-fold helices due to the bulky guest compound (Yamashita & Monobe, 1971).

The central cavity of V-amylose single helices is hydrophobic and can host various inorganic and organic molecules (Tomasik, Schilling, & Derek, 1998b, 1998a), so the hosting ability of V-amylose can be applied as targeted and controlled delivery of various substances. Also, the encapsulation of guest compounds by formation of inclusion complexes leads to stabilization of the guest compounds, due to protection against the influence of oxygen or light (Wulff, Avgenaki, & Guzmann, 2005). Thus, molecular inclusions in V-amylose complexes may be used for encapsulation and controlled delivery of various substances in the pharmacology

* Corresponding author. Tel.: +82 2 3290 3435; fax: +82 2 921 0557.
E-mail addresses: tvand@paran.com (J.-Y. Kim), limst@korea.ac.kr (S.-T. Lim).

0144-8617/$ – see front matter © 2010 Elsevier Ltd. All rights reserved.
doi:10.1016/j.carbpol.2010.04.050

and food industry. In addition, application of nanotechnology to the delivery of various biofunctional substances has attracted much attention due to its great potential in improving the efficiency of the bioactive compounds (Chen, Weiss, & Shahidi, 2006). In delivery systems, a comprehensive understanding of physicochemical properties, such as particle size or morphology of the delivery agent, is imperative. Although the physicochemical properties of V-amylose have already been extensively studied, it is not yet fully understood how the size and morphology of V-amylose crystals are affected by the parameters for complex formation such as temperature, chain structure of amylose, concentration of amylose in solution, and the type of guest molecules. V-amylose crystals are normally formed by complex formation with guest compounds as micrometer-sized particles, and overall morphology of the particles is highly dependent on the guest molecules and production method (Lesmes, Cohen, Shener, & Shimoni, 2009). Only a few studies (Kim, Yoon, & Lim, 2009) have been conducted on the preparation of nano-sized V-amylose particles.

In this study, V-amylose complexes were prepared through the interaction between a dextrin in an aqueous solution and *n*-butanol as separated phases. The particle size, morphology, crystalline characteristics, molecular structure and yield of the complex particles were investigated in various physicochemical conditions for the complex formation.

2. Materials and methods

2.1. Materials

Amylomaize starch (Hylon VII, 70% amylose) was provided from National Starch and Chemical Company (Bridgewater, NJ, USA). Isoamylase (EC 3.2.1.68, activity 1122 units/mg) was purchased from Hayashibara Co., Ltd. (Okayama, Japan).

2.2. Preparation of dextrin

A dextrin was prepared following the method of Kim et al. (2009). The amylomaize starch was hydrolyzed in an acid alcohol solution (HCl and ethyl alcohol) at 20 °C for 72 h. The dextrin was purified using an aqueous DMSO solution (90%) and absolute ethyl alcohol (Klucinec & Thompson, 1998). The number-average degree of polymerization (DP_n) of the dextrin was 311 by calculating the ratio between reducing value and total carbohydrate content (DuBois, Gilles, Hamilton, Rebers, & Smith, 1956; Jane & Robyt, 1984; Somogyi, 1952).

2.3. Preparation of complexes

The dextrin (1.0–3.0%, w/v) was dispersed in distilled water (20 mL) and the suspension was heated at 131 °C for 20 min. The dextrin solution was cooled to 70 °C and an aliquot (5 mL) of *n*-butanol was slowly added to the dextrin solution to form a separated butanol phase from the dextrin solution. The dextrin solution was then stirred gently (0–150 rpm) at 25–70 °C for 6 days. At regular intervals, the dextrin solution was collected by centrifugation (20,000 × *g*, 10 min), and then the precipitates were dried at 121 °C. The weight of the precipitates was measured to calculate the yield of the dextrin complex obtained as precipitates. The supernatant was also collected for further analysis of the chain profile of the dextrin that had not been used for complex formation.

2.4. X-ray diffraction pattern (XRD)

At regular intervals during complex formation, aliquots of the dextrin solution were taken and the complex was collected by centrifugation (20,000 × *g*, 10 min). The precipitated complex was then dried in a speed vacuum dryer (N-biotek, Bucheon, Korea) at 40 °C. The crystalline structure of the dried complex was determined using an X-ray diffractometer (MAC Science Co., Japan) at a target voltage and current of 40 kV and 40 mA, respectively. The scanning range and rate were 3–30° (2θ) and 1.0° min^{-1}, respectively.

2.5. Transmission electron microscopy (TEM)

The dextrin complex (0.3 mg) was suspended in distilled water (1 mL), and a drop of the suspension was deposited on a carbon-coated microscopy grid. It was negatively stained with a drop of 2% (w/v) uranyl acetate, dried at room temperature, and imaged using a transmission electron microscope (Philips Tecnai 12, Eindhoven, Netherlands).

2.6. Particle size distribution

The hydrodynamic particle size of the complex particles was determined using a dynamic light scattering detector (Dynapro Titan, Wyatt Technology, Santa Barbara, CA) using a Dynamics program (Version 6.9.2.9, Wyatt Technology, Santa Barbara, CA). The complex particles collected by centrifuging the dextrin solution were re-dispersed in distilled water and the size distribution was analyzed. The refractive index and the viscosity of water, determined using the calculation software, were 1.333 and 1.00 cP at 20 °C, respectively.

2.7. Molecular size of dextrin chains

The molecular sizes of dextrin in the complex and that remaining in supernatant after centrifugation were measured using a high-pressure size exclusion chromatography (HPSEC) with TSK G5,000 PWXL column (Tosoh Bioscience, Montgomeryville, PA, USA), monitored by a refractive index detector (Shodex RI-71, Tokyo, Japan). The free dextrin (dextrin remaining in supernatant) and the dextrin in the complex (about 2 mg, dry basis) were dissolved in 1 N NaOH solution (1 mL) by vortexing, and the solutions were diluted with 50 mM $NaNO_3$ (3 mL). After neutralizing with 1 N HCl, the solutions were autoclaved (121 °C, 20 min) for dissolution, and then filtered through a membrane filter (5.0 μm; Pall Gelman Sciences, Ann Arbor, MI, USA) prior to the HPSEC analysis. Dextran standards of different molecular weights (2,000,000, 500,000, 70,000, and 10,000) were used to calculate the molecular sizes of the dextrins. The mobile phase was a 50 mM $NaNO_3$ solution containing 0.02% NaN_3 and the flow rate was 0.4 mL/min.

The chain profiles of the amylomaize starch and dextrins were measured after debranching with an isoamylase using a high-pressure size exclusion chromatography (HPSEC) with Superdex 75 10/300 GL (Amersham Pharmacia Biotech, Uppsala, Sweden), monitored by a refractive index detector (Shodex RI-71, Tokyo, Japan). The purified dextrin was dispersed in 50 mL of water and then autoclaved at 121 °C for 15 min for dissolution. To debranch the dextrin, an acetate buffer (0.1 M, pH 3.5, 400 μL) and isoamylase (2 μL, 2,900 unit/mL) were added to the dextrin solution, and the mixture was incubated at 45 °C for 24 h. The enzyme was inactivated by boiling the solution for 15 min. The solution was filtered through a glass filter and then filtered again through a membrane filter (5.0 μm; Pall Gelman Sciences, Ann Arbor, MI, USA) prior to the HPSEC analysis. Pullulan standards (112,000, 47,300, 22,800, 11,800, 5,900, and 667) were used to calculate the chain lengths of the dextrins. The mobile phase was distilled water and the flow rate was 0.4 mL/min.

Table 1
Chain profiles of amylomaize starch and dextrin (DP 311).

	Fraction (F) of dextrin chains[a]				
	F-1	F-2	F-3	F-4	F-5
Amylomaize starch					
CL_w[b]	1100.68 ± 1.51	228.09 ± 23.55	53.35 ± 3.36	29.10 ± 3.39	14.71 ± 1.30
%	37.39 ± 0.06	16.85 ± 4.72	34.62 ± 4.70	4.26 ± 1.45	6.87 ± 1.48
Dextrin					
CL_w[b]	1040.00 ± 3.56	–	62.84 ± 9.34	35.52 ± 2.24	14.51 ± 0.37
%	33.88 ± 0.54	–	47.29 ± 0.89	5.14 ± 0.11	13.21 ± 0.54

[a] The fraction number indicates the group of chains based on size.
[b] CL_w is weight average chain length.

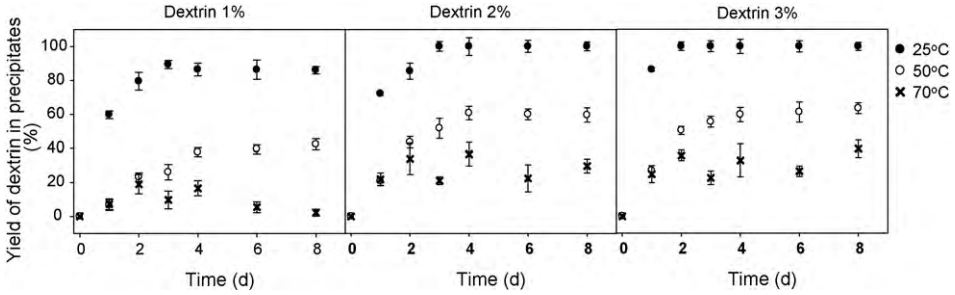

Fig. 1. Yield of dextrin in the precipitated complex at different dextrin concentrations and temperatures for complex formation (25–70 °C).

3. Results and discussion

3.1. Chain profile of dextrin

The dextrin prepared by hydrolyzing amylomaize starch in an acidic alcohol solution showed an average DP_n value of 311, but the granule shape of the starch remained (data not shown). The native amylomaize starch consisted of 5 chain fractions based on chain length (Table 1). The fraction of the largest chains (F-1) might be originated from amylose. Considering that the amylomaize starch contained 70% amylose, it was supposed that some of the amylose chains existed in the fractions of smaller chains, possibly in F-2 and F-3. The fractions of short chains such as F-3, -4, and -5, however, might consist of amylopectin chains, so called A and B chains. After the hydrolysis for dextrin preparation, the chain length and proportion of the F-1 fraction were slightly decreased and the F-2 fraction was disappeared (Table 1). With these changes, the chain length and proportion of the small chains (F-3, -4 and -5) were increased, indicating that amylose and long amylopectin chains (F-1 and -2) were the major starch chains subjected to acid hydrolysis, resulting in the production of shorter chain fractions (F-3, -4 and -5).

3.2. Formation of dextrin-butanol complex

Preparation of the dextrin–butanol complex was possible by using separated phases of aqueous dextrin and *n*-butanol. The solubility of *n*-butanol in aqueous solvent is 6–8% at a temperature lower than 80 °C (Aoki & Moriyoshi, 1978). Therefore, excessive *n*-butanol added to the aqueous dextrin solution caused a phase separation of butanol against the aqueous solution, residing in upper phase due to the lower density of *n*-butanol (0.8098 g/cm^3 at 25 °C) than that of water. The aqueous dextrin solution was quickly saturated with *n*-butanol and the dissolved *n*-butanol could readily form the complex with dextrin. Subsequently *n*-butanol dissolved in the dextrin solution was continually consumed as the complex was formed. Simultaneously same amount of *n*-butanol was expected to migrate from the upper layer continuously into the dextrin solution, and thus the formation of the dextrin–butanol complex proceeded continuously. Actually the butanol content in the dextrin solution reached an equilibrium at approximately 6% while the complex was formed (data not shown).

The complex in the dextrin solution tends to gradually aggregate, producing large particles which could be precipitated by centrifugation. Based on the amount of precipitates, the complex formation appeared proceeding rapidly during initial 2–4 days of storage, and then reached a plateau afterward (Fig. 1). The maximum amount of the precipitates depended on the dextrin concentration and temperature. As the dextrin concentration was higher and temperature for complex formation was lower, the yield of precipitates was higher. However, the higher yield did not assure the higher crystallinity. At 25 °C, almost all of the dextrin used was recovered as precipitates, but the analysis using an X-ray diffraction revealed that the precipitates at 25 °C had mainly amorphous matrices (data not shown), showing no presence of the V-type crystal. The association between dextrin chains occurred more readily as the temperature was lower, and the rapid association between the dextrin chains might result in the formation of an amorphous network. As the temperature for complex formation increased, the amount of recovered precipitates was reduced. At 50 °C, 40–60% of the dextrin in the solution was recovered as precipitates, and the yield slightly increased as the dextrin concentration increased. X-ray diffraction analysis of the precipitates revealed that the precipitates at a high dextrin concentration (2 or 3%) contained mainly B-type crystals, whereas that at 1% dextrin concentration contained V-type crystals (data not shown). The association between dextrin chains was hindered by raising temperature because of the increase chain mobility. Therefore the increase in temperature to 50 and 70 °C reduced the amount of precipitates. It was assumed that the dissolution of some *n*-butanol decreased the dextrin solubility, which thus assisted the association between dextrin chains. The dextrin–dextrin association should be restricted for more dextrin chains to interact with butanol and form complex. When dextrin content was high (2 and 3% in this study), more physical contact between the dextrin chains became available, consequently forming mainly B-type crystals. In contrast, interactions between dextrin chains became less in a diluted solution (1% dextrin), and more butanol was allowed to form complex with dextrin chains, resulting the V-type crystalline precipitates. Therefore, using a

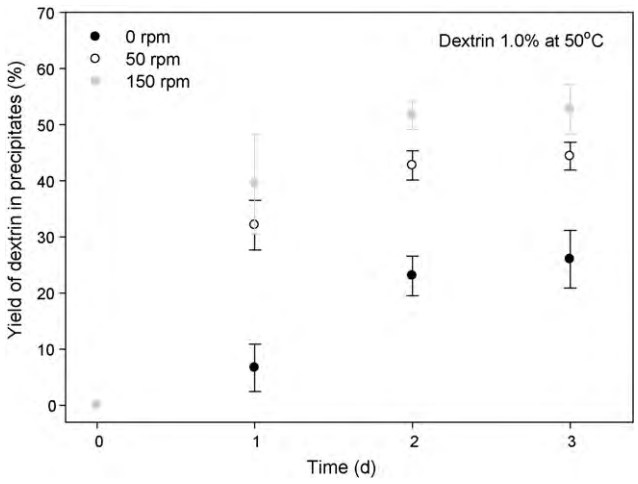

Fig. 2. Yield of dextrin in the precipitated complexes from 1.0% dextrin solution after complex formation at 50 °C for 3 days at different stirring speeds.

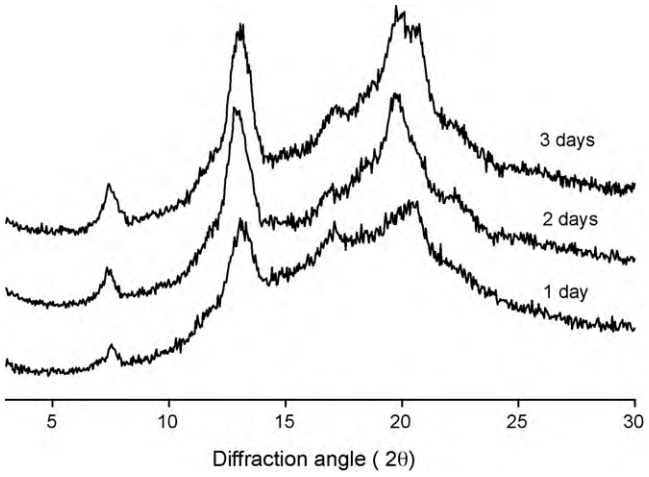

Fig. 3. X-ray diffraction patterns of the complexes from 1.0% dextrin solution after complex formation at 50 °C.

sufficiently dilute dextrin solution with mild heating was kinetically favored for the complex formation with butanol containing V-type crystals.

At the highest temperature tested (70 °C), the precipitates formed during the initial 2 days appeared similar to those observed at 50 °C. The amount of precipitates, however, was less than that at 50 °C. The increased chain mobility by raising temperature (70 °C) might have induced the decrease in the dextrin association and *n*-butanol or dextrin complex formation, resulting in the low recovery of the precipitates.

During the complex formation, mechanical treatment was applied to increase the yield of the complex. Mild stirring (50 and 150 rpm) of the dextrin solution induced increases in complex formation and yield of precipitates (Fig. 2). Physical interaction between dextrin chains and *n*-butanol was enhanced by the magnetic stirring, resulting in increased amount of complex. Consequently dextrin–butanol complex was obtained at a yield higher than 50% and in V-type crystal form when 1% dextrin solution reacted with *n*-butanol at 50 °C with a proper stirring (150 rpm). Stirring at higher rate than 150 rpm, however, was not effective in increasing the yield (data not shown).

3.3. X-ray diffraction

The X-ray diffraction patterns of the complexes prepared by stirring (150 rpm) the dilute dextrin solution (1.0%) at 50 °C for different periods are presented in Fig. 3. The complexes exhibited a V_H pattern with 3 diffractions at *d*-spacings 1.123, 0.657, and 0.429 nm (7.57, 13.08, and 20.71° in 2θ) with a minor B pattern (reflection at 17.34° in 2θ). Previous studies reported that amylose might form a complex with *n*-butanol entrapped not only within the helices but also in the space between the helices (Helbert & Chanzy, 1994; Le Bail, Rondeau, & Buléon, 2005). However, the complexes prepared in this study yielded only the V_H complex in which butanol was entrapped only within the helices. It was assumed that a transformation from $V_{butanol}$ to V_H had occurred during the drying process of the precipitates for X-ray diffraction analysis. Evaporation of the butanol molecules located between the helices might allow the transformation to V_H crystal (Le Bail et al., 2005). The intensity of the diffractions at *d*-spacings 1.123, 0.657, and 0.429 nm was increased as the period for the complex formation was extended to 3 days.

3.4. Hydrodynamic size distribution and morphology of complexes

Hydrodynamic particle size distribution of the complexes prepared with a dilute (1.0%) dextrin solution reacted at 50 °C for 3 days are presented in Fig. 4. The complexes showed two different fractions in size distribution: a fraction from 100 to 200 nm and micro-sized fraction. The large particles represented the aggregates of the nano-sized complexes. When the complex formation

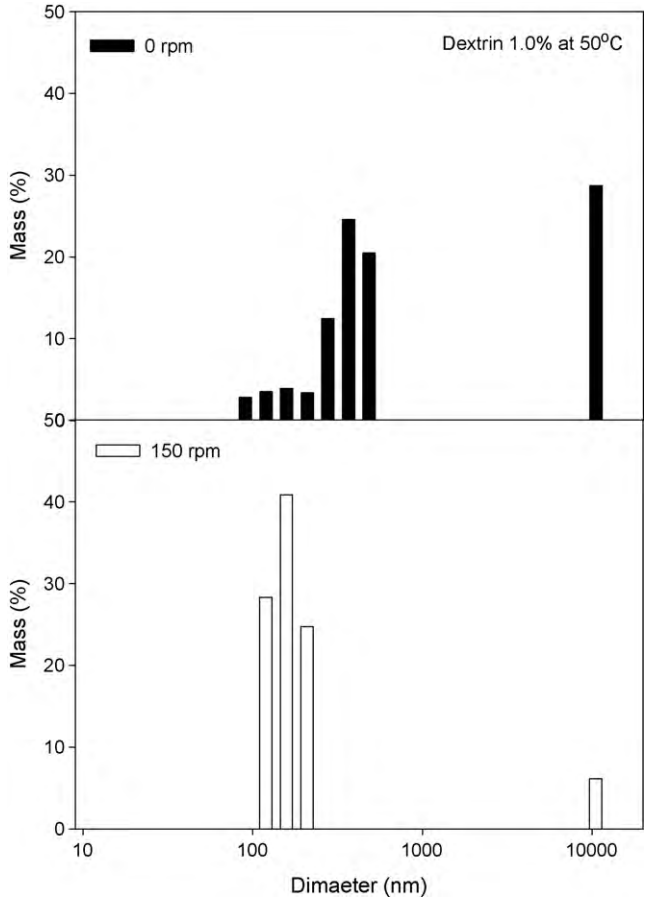

Fig. 4. Particle size distribution of the complexes from 1.0% dextrin solution after complex formation at 50 °C for 3 days.

was performed with stirring (150 rpm), a less amount of aggregates was formed and more particles were produced in nano-size (94%), which indicated that the stirring had hindered aggregation of the complex particles. Also this distribution pattern demonstrates that the stirring during the complex formation made the complex particles more homogeneous in size.

Assembly of particles or molecules to form aggregates relies on balancing the forces of attraction and repulsion between a pair of particles or molecules, and these forces can be influenced by mechanical treatments such as shear (Sanguansri & Augustin, 2006). Actually assembly of amylose molecules during reorganization is influenced by shear (Gidley & Bulpin, 1989), as provided in the previous data (Fig. 2). V-type crystals induced by amylose are usually obtained in a lamellae structure that is assembled by the lateral stacking of single helical units by hydrogen bonds (Brisson et al., 1991; Manley, 1964). Addition of urea during complex formation without stirring caused a reduction in size of the complex (50–130 nm), because urea disrupted hydrogen bonds (He, Fu, Shen, & Gao, 2008). Therefore, disruption of hydrogen bonds could reduce the size of the complex particles, by either using chemicals or physical forces. Thus, the stirring during the complex formation reduced the formation of micro-sized aggregates (Fig. 4).

Fig. 5 shows a transmission electron microscopic (TEM) image of the dextrin–butanol complex prepared using a 1.0% dextrin solution at 50 °C with stirring (150 rpm) for 3 days. The complex exhibited rectangular shaped platelets in similar shape to those reported for the amylose–butanol complex (Booy et al., 1979; Manley, 1964); however, the size of the particles was smaller than those reported for the amylose–butanol complex. Most of the complex particles in the TEM image were smaller than 200 nm (Fig. 5). There were differences between the size distribution data from the light scattering analysis and those from TEM images. The hydrodynamic diameter measured by light scattering is a particle radius that embodies a hard sphere particles, in fact, aspherical, and typically surrounded by solvent, whereas those for TEM observation were in dried state.

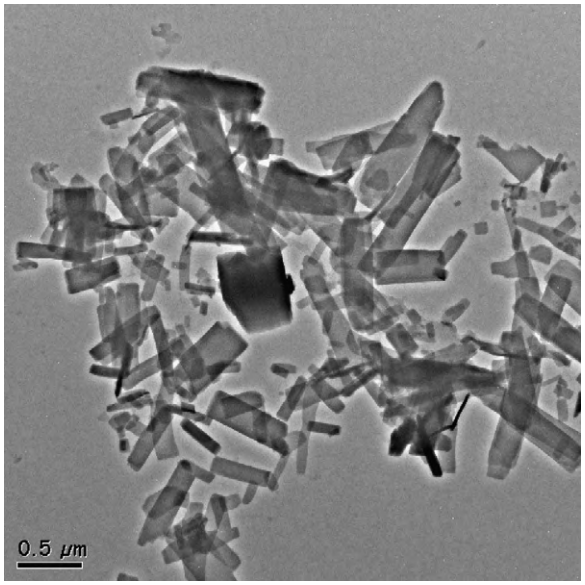

Fig. 5. Transmission electron micrograph of a negatively stained dextrin–butanol complex from 1.0% dextrin solution after complex formation at 50 °C for 3 days.

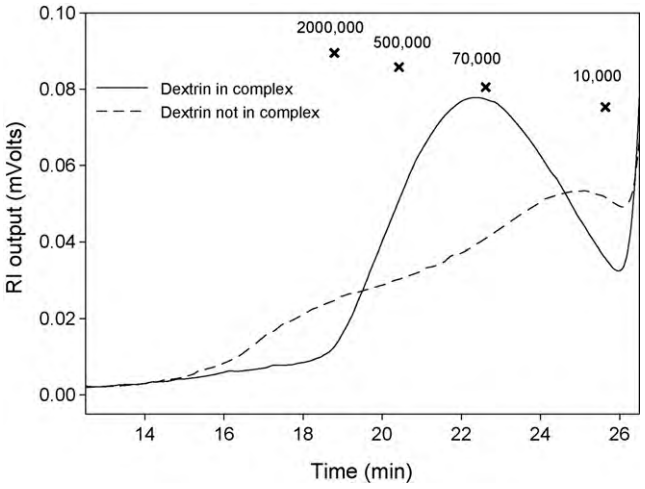

Fig. 6. Molecular size distributions of the dextrins in complex and in supernatant (not in complex) from 1.0% dextrin solution after complex formation at 50 °C for 3 days.

3.5. Molecular properties of dextrins

Molecular size of the dextrin participated in complex formation and the dextrin remained in the supernatant after centrifugation was investigated (Fig. 6). The dextrin incorporated in the complex had an average molecular size of about 100,000. In contrast, the dextrin that was not used for complex formation had a wider range of size. It was revealed that the dextrin chains of too large or too small sizes were not able to form complex. The chain profiles of the dextrin in the complex and in the supernatant were compared (Table 2). The dextrin in the complex showed higher chain length with more than 100 anhydroglucose units (F-1, -2, and -3), whereas the dextrin not in the complex mainly contained short chains (F-4 and -5). It was hypothesized that the large dextrin chains that had not been consumed for complex formation (Fig. 6) might originate from large amylopectin molecules which were highly branched with small chains as shown in F-4 and F-5 fractions. The small dextrins that were not consumed for complex formation might be the dextrins produced from amylose or amylopectin, but the chain length was not long enough to form the complex with butanol. It

Table 2
Chain profiles of dextrins in a complex.

Dextrin	Fraction (F) of dextrin chain[a]				
	F-1	F-2	F-3	F-4	F-5
In complex					
CL_w[b]	1004.24 ± 39.91	220.23 ± 0.68	102.65 ± 3.11	–	–
%	69.62 ± 3.58	21.04 ± 2.59	7.21 ± 1.48	–	–
Not in complex					
CL_w[b]	883.55 ± 31.47	–	84.25 ± 6.71	46.31 ± 0.30	15.98 ± 0.60
%	8.72 ± 0.88	–	15.02 ± 1.41	39.00 ± 0.81	37.26 ± 1.49

[a] The fraction number indicates the group of chains based on size.
[b] CL_w is weight average chain length.

was supposed that the dextrin chains that were able to form complex with butanol were produced from mainly amylose, which had chain length and linearity favorable for complex formation (Godet, Bizot, & Buléon, 1995).

4. Conclusion

Crystalline dextrin particles could be prepared by complex formation between an amylomaize dextrin (DP_n 311) and *n*-butanol using a phase separation method. Minimizing dextrin–dextrin association with mild heating and stirring in a sufficiently diluted solution was needed for efficient complex formation containing V-type crystals. The rectangular nano-sized complex particles mainly consisted of V_H crystals, the size of which ranged from 100 to 200 nm. Mainly long amylose chains appeared participating in the formation of complex. The complex particles could be useful as vehicles for encapsulation and controlled delivery of various substances.

References

Aoki, Y., & Moriyoshi, T. (1978). Mutual solubility of n-butanol + water under high pressures. *The Journal of Chemical Thermodynamics*, *10*(12), 1173–1179.

Booy, F. P., Chanzy, H., & Sarko, A. (1979). Electron diffraction study of single crystals of amylose complexed with *n*-butanol. *Biopolymers*, *18*(9), 2261–2266.

Brisson, J., Chanzy, H., & Winter, W. T. (1991). The crystal and molecular structure of V_H amylose by electron diffraction analysis. *International Journal of Biological Macromolecules*, *13*(1), 31–39.

Buléon, A., Delage, M. M., Brisson, J., & Chanzy, H. (1990). Single crystals of V amylose complexed with isopropanol and acetone. *International Journal of Biological Macromolecules*, *12*(1), 25–33.

Cardoso, M. B., Putaux, J.-L., Nishiyama, Y., Helbert, W., Hytch, M., Silveira, N. P., et al. (2007). Single crystals of V-amylose complexed with α-naphthol. *Biomacromolecules*, *8*(4), 1319–1326.

Chen, H., Weiss, J., & Shahidi, F. (2006). Nanotechnology in nutraceuticals and functional foods. *Food Technology*, *60*(3), 417–425.

DuBois, M., Gilles, K. A., Hamilton, J. K., Rebers, P. A., & Smith, F. (1956). Colorimetric method for determination of sugars and related substances. *Analytical Chemistry*, *28*(3), 350–356.

Gidley, M. J., & Bulpin, P. V. (1989). Aggregation of amylose in aqueous systems: The effect of chain length on phase behavior and aggregation kinetics. *Macromolecules*, *22*(1), 341–346.

Godet, M. C., Bizot, H., & Buléon, A. (1995). Crystallization of amylose—Fatty acid complexes prepared with different amylose chain lengths. *Carbohydrate Polymers*, *27*(1), 47–52.

Godet, M. C., Tran, V., Delage, M. M., & Buléon, A. (1993). Molecular modelling of the specific interactions involved in the amylose complexation by fatty acids. *International Journal of Biological Macromolecules*, *15*(1), 11–16.

He, Y., Fu, P., Shen, X., & Gao, H. (2008). Cyclodextrin-based aggregates and characterization by microscopy. *Micron*, *39*(5), 495–516.

Helbert, W., & Chanzy, H. (1994). Single crystals of V amylose complexed with n-butanol or n-pentanol: Structural features and properties. *International Journal of Biological Macromolecules*, *16*(4), 207–213.

Hulleman, S. H. D., Helbert, W., & Chanzy, H. (1996). Single crystals of V amylose complexed with glycerol. *International Journal of Biological Macromolecules*, *18*(1/2), 115–122.

Imberty, A., Chanzy, H., Pérez, S., Buléon, A., & Tran, V. (1988). The double-helical nature of the crystalline part of A-starch. *Journal of Molecular Biology*, *201*(2), 365–378.

Imberty, A., & Perez, S. (1988). A revisit to the three-dimensional structure of B-type starch. *Biopolymers*, *27*(8), 1205–1221.

Jane, J.-L., & Robyt, J. F. (1984). Structure studies of amylose-V complexes and retrograded amylose by action of alpha amylases, and a new method for preparing amylodextrins. *Carbohydrate Research*, *132*(1), 105–118.

Kim, J.-Y., Yoon, J.-W., & Lim, S.-T. (2009). Formation and isolation of nanocrystal complexes between dextrins and n-butanol. *Carbohydrate Polymers*, *78*(3), 626–632.

Klucinec, J. D., & Thompson, D. B. (1998). Fractionation of high-amylose maize starches by differential alcohol precipitation and chromatography of the fractions. *Cereal Chemistry*, *75*(6), 887–896.

Le Bail, P., Rondeau, C., & Buléon, A. (2005). Structural investigation of amylose complexes with small ligands: Helical conformation, crystalline structure and thermostability. *International Journal of Biological Macromolecules*, *35*(1/2), 1–7.

Lesmes, U., Cohen, S. H., Shener, Y., & Shimoni, E. (2009). Effects of long chain fatty acid unsaturation on the structure and controlled release properties of amylose complexes. *Food Hydrocolloids*, *23*(3), 667–675.

Manley, R. S. J. (1964). Chain folding in amylose crystals. *Journal of Polymer Science Part A: General Papers*, *2*(10), 4503–4515.

Nuessli, J., Putaux, J. L., Bail, P. L., & Buléon, A. (2003). Crystal structure of amylose complexes with small ligands. *International Journal of Biological Macromolecules*, *33*(4/5), 227–234.

Putaux, J.-L., Cardoso, M. B., Dupeyre, D., Morin, M., Nulac, A., & Hu, Y. (2008). Single crystals of V-amylose inclusion complexes. *Macromolecular Symposia*, *273*(1), 1–8.

Rappenecker, G., & Zugenmaier, P. (1981). Detailed refinement of the crystal structure of Vh-amylose. *Carbohydrate Research*, *89*(1), 11–19.

Sanguansri, P., & Augustin, M. A. (2006). Nanoscale materials development—A food industry perspective. *Trends in Food Science & Technology*, *17*(10), 547–556.

Somogyi, M. (1952). Notes on sugar determination. *Journal of Biological Chemistry*, *195*(1), 19–23.

Tomasik, P., Schilling, C. H., & Derek, H. (1998a). *Complexes of Starch with Inorganic Guests. Advances in Carbohydrate Chemistry and Biochemistry*. Academic Press., pp. 263–343.

Tomasik, P., Schilling, C. H., & Derek, H. (1998b). *Complexes of Starch with Organic Guests. Advances in Carbohydrate Chemistry and Biochemistry*. Academic Press., pp. 345–426.

Welland, E. L., & Donald, A. M. (1991). Single crystals of V amylose. *International Journal of Biological Macromolecules*, *13*(2), 69–72.

Whittam, M. A., Orford, P. D., Ring, S. G., Clark, S. A., Parker, M. L., Cairns, P., et al. (1989). Aqueous dissolution of crystalline and amorphous amylose–alcohol complexes. *International Journal of Biological Macromolecules*, *11*(6), 339–344.

Wulff, G. T., Avgenaki, G., & Guzmann, M. S. P. (2005). Molecular encapsulation of flavours as helical inclusion complexes of amylose. *Journal of Cereal Science*, *41*(3), 239–249.

Yamashita, Y., & Monobe, K. (1971). Single crystals of amylose V complexes. III. Crystals with 8_1 helical configuration. *Journal of Polymer Science Part A-2: Polymer Physics*, *9*(8), 1471–1481.